Effect of temperature on the formation and dissolution of anodic oxide films on titanium in acid solutions

A. A. MAZHAR

Chemistry Department, Faculty of Science, Cairo University, GIZA, Egypt

The effect of electrolyte and current density on the growth rate of the oxide film on titanium were studied by following the voltage–time characteristics. The barrier oxide grows to greater thickness at lower pH and higher current density. The growth of the oxide in acid medium is lowered by an increase in temperature. In $0.5\,N\,H_2SO_4$ the oxide grows to greater thicknesses than that grown in $0.5\,N\,HClO_4$. This is due to a relatively higher rate of dissolution in $HClO_4$ during the oxide-growth/oxide-dissolution process during the anodization. The effect of temperature on the dissolution of the oxide previously grown to 12.5 V is followed in $0.5\,N\,H_2SO_4$ by impedance and potential measurements. The oxide, which is of duplex nature, dissolves with a rate that increases with increasing temperature. The results indicate that the rate of dissolution of the outer layer is affected by temperature more than that of the inner layer, probably owing to higher porosity of the former. The heat of activation, $-\Delta H$, was estimated to be $110.5\,kJ\,mol^{-1}$.

1. Introduction

Metal oxides are compounds of variable composition, especially when the metal ion can exist in more than one oxidation state as with Ti [1, 2]. Ample evidence indicates that films prepared on titanium in aqueous electrolytes are not of the pure rutile structure [3]. Previous studies showed that the anodic oxide film formed on Ti is of duplex nature [4–6]. The inner barrier layer consists of the rutile oxide while the outer is of the amorphous oxide. The rate of dissolution of the oxide was found to follow a zero order mechanism in H_2SO_4 [4], that is, the rate does not depend on the thickness of the remaining oxide.

Andreeva employed an optical polarization technique to follow the film thickening in H_2SO_4 and Na_2SO_4 while varying the potential of the metal [7]. Titanium oxide films of various porosities were obtained under different polarization conditions by Sibert [3] and by Ence and Margolin [8].

Studies on the growth of ZrO_2 showed that the onset of corrosion, termed breakdown, manifests itself as a decrease in the slope of the voltage–time curves for anodization at a constant current. At the breakdown potential, slower growth of the barrier film continues, together with the rapid growth of an adherent but non-protective product [9]. Previously, Breiter found that the oxide films on Ti begin to break down in the potential range 11.5 to 14.5 V in HCl solutions [10]. Anions present in the electrolytic solution restrict the development of the barrier films to certain potentials, while the c.d., which can alter the local concentrations of ions, affects the dissolution behaviour of the oxide. This study is concerned with the development of anodic oxide films on Ti and the effect of temperature on its dissolution in H_2SO_4.

2. Experimental details

Several techniques are available for examining the properties of the outer surface of oxide films and the defects therein. The capacitance method has been recommended and used for examination of these properties [11]. The electrical circuit and the cell are the same here as used previously [5, 6, 12]. The electrode was made from 99.9% Ti rod (Imperial Metal Industries (Kynoch) Ltd), fixed in a glass tube. The cross-sectional area of the electrode was $0.07\,cm^2$. The electrolytes used were H_2SO_4, $HClO_4$ and NaOH prepared from Analar grade chemicals and redistilled water. The solutions were naturally aerated. The temperature was adjusted to within $\pm 0.1^\circ C$. The electrode was mechanically polished as described previously [12]. The electrode was left immersed in the test solution for 30 min before applying the anodic current.

The capacitance (C_m) and resistance (R_m) of the oxide film were measured after various periods of immersion at a fixed frequency of 1 KHz. To obtain the most reproducible results time was allowed for thermal equilibrium to be reached. The first readings were taken after 5 min. Open-circuit potential measurements were always made while the leads to the a.c. bridge were disconnected. Potential, e_h, was measured against the SCE and then referred to the NHE.

3. Results and discussion

3.1. Growth of anodic oxides on Ti

The growth rate during anodization was determined by monitoring the voltage rise with time (V–t curves) in $0.5\,N$ solutions of H_2SO_4 and NaOH at a c.d. of $7.14\,mA\,cm^{-2}$, as shown in Fig. 1. The ability to form
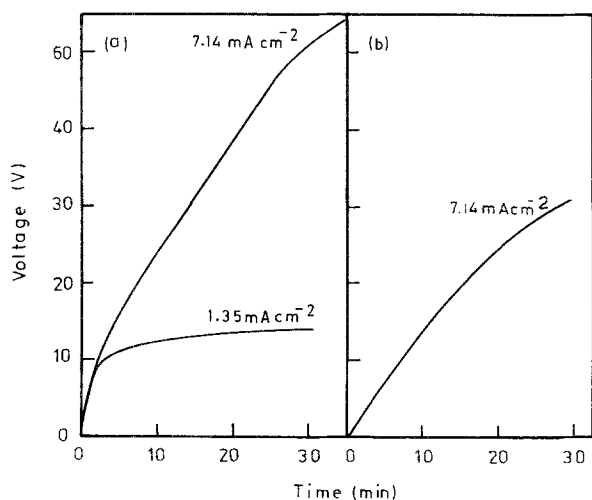
Fig. 1. Effect of medium and c.d. on the breakdown of TiO_2: (a) 0.5 N H_2SO_4; (b) 0.5 N NaOH.

a barrier layer up to high voltages depends on the growth rate and on the bulk pH [9]. The figure shows that the growth rate under the same anodizing conditions is higher in H_2SO_4. It is known that Ti oxide dissolves more easily in caustic solutions than in acid solutions [5, 13]. It has been shown that the oxide thickness under open circuit conditions drops abruptly after 30 min immersion in NaOH [4]. The figure shows a gradual change in dV/dt rather than a breakdown, which indicates a decrease in the rate of total oxide thickening, especially in NaOH. Figure 1a shows the effect of c.d. on the growth of the oxide. It is clear that a rapid change in dV/dt is observed at lower c.d. This occurs at a lower potential as observed previously in anodizing Zr in borate electrolytes [14]. There is a very small increase in potential with time which suggests that there is a very limited increase in the barrier film thickness, although the total film thickness continues to grow, probably at a higher rate. The effect of c.d. is probably brought about through alteration of the local concentration of ions, resulting in a change in the pH at the surface [9].

The effect of temperature on V/t curves in 0.5 N H_2SO_4 at 7.14 mA cm^{-2} is shown in Fig. 2. The decrease in the rate of voltage rise (dV/dt), observed during anodizing at each temperature, occurs because of breakdown of the oxide film. There is a decrease in dV/dt with increase in temperature, the breakdown meanwhile occurring at lower potentials. There is no further increase in potential after breakdown, as clearly shown at 45° and 55° C. This suggests that under these conditions a constant barrier film thickness is reached, although the total film thickness may increase. The change in behaviour at the breakdown potential results in a slower growth rate of the barrier films at 25° and 35° C. In all cases the rapid growth of the non-protective outer layer continues. Similar observations were reported in the case of anodizing Zr [14]. The barrier layer grows to higher voltages at lower temperatures.

The dV/dt characteristics do not depend only on pH and temperature, as shown in Fig. 3 which depicts the dependence of the growth rate in 0.5 N $HClO_4$ at 5.0 mA cm^{-2} on temperature. The figure reveals that a limited variation in temperature does not affect the breakdown voltage in $HClO_4$ ($\simeq$ 14 V), as compared with 11.5 to 14.5 V in HCl reported by Breiter [10]. After breakdown the voltage drops over the same time interval and remains nearly constant at potentials decreasing with increase in temperature. Then it drops again over the same time interval to a potential that decreases with increase in temperature. Fluctuations in potential are observed after reaching the breakdown potential. After breakdown, the abrupt thickening of the film is attributed to the creation of lattice defects which increase the ionic leakage current [15]. After breakdown a porous oxide is formed. The breakdown results from critically large tensile stresses in the oxide [14], probably brought about by incorporation of trace quantities of ClO_4^- ions. Before breakdown the ClO_4^- ions incorporated into the oxide do not alter the field strength or the c.d. and thus the growth rate is unaffected [14, 16]. After
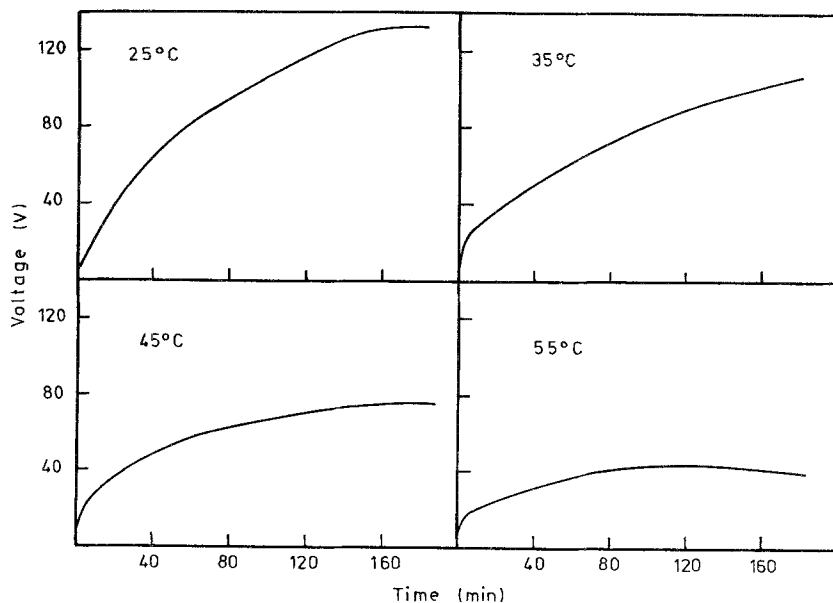

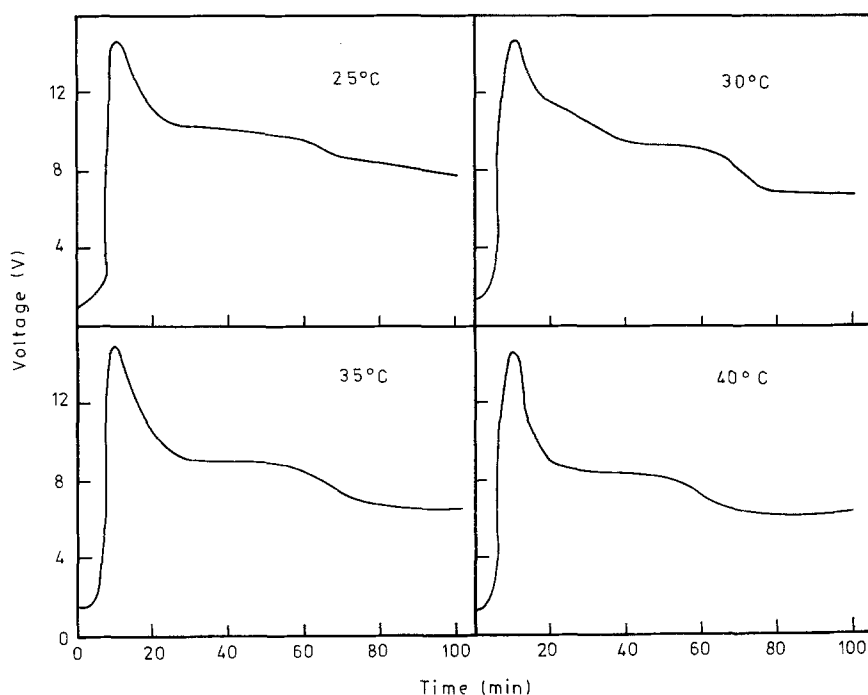Fig. 2. Effect of temperature on the breakdown of TiO_2 in 0.5 N H_2SO_4 at 7.14 mA cm^{-2}.

Fig. 3. Effect of temperature on the breakdown of TiO_2 in 0.5 N $HClO_4$ at 5.0 mA cm^{-2}.

breakdown the proportion of current used to grow the porous layer decreases with increase in temperature as observed in Fig. 3, so that the total thickness of oxide continually increases. The oxides formed at higher temperature are probably more porous. In general, the figure shows that the barrier layer thickness in $HClO_4$ is less than that in H_2SO_4 [5, 6]. This may be due to the aggressiveness of this electrolyte as observed in the dissolution of Al [17]. The dissolution may be related to the smaller size of the ClO_4^- ion, leading to comparatively easy incorporation into the formed oxide.

3.2. Effect of temperature on the dissolution of anodic oxide films on Ti in H_2SO_4

Anodic oxide films were formed on Ti in 0.5 N H_2SO_4 solutions at 2.04 mA cm^{-2} at 25° C up to 12.5 V. The barrier oxide formed on Ti to 12.5 V was observed to be the thickest and most stable [4, 5]. After reaching this potential, the applied current was interrupted and the impedance of the surface oxide film was followed as a function of time in fresh solutions of 0.5 N H_2SO_4. Figures 4 and 5 show the measured capacitance and

resistance plotted against the square root of time for a period of 3 h, which is the duration of the dissolution experiments. Both C_m^{-1} and R_m decrease with the square root of time and with temperature. C_m^{-1} is considered to be a direct function of oxide thickness [10].

These results imply that the surface oxide film dissolves in 0.5 N H_2SO_4. The dependence of C_m^{-1} on $t^{1/2}$ can be expressed by the relation

$$C_m^{-1} = \alpha - \beta t^{1/2} \qquad (1)$$

where α and β are constants, α equals C_m^{-1} at zero time and β is the rate coefficient for the dissolution process. The figure also reveals that the rate of dissolution increases with increasing temperature, which shows that dissolution is probably of a purely chemical nature.

The change in the slope of the two straight lines in Fig. 4 indicates a change in the mechanism of the dissolution process. This is in agreement with previous observations of the duplex nature of the film [5, 6]. Oxides of metals exhibiting more than one oxidation state are likely to be composed of layers of oxides differing in their chemical and electrochemical nature
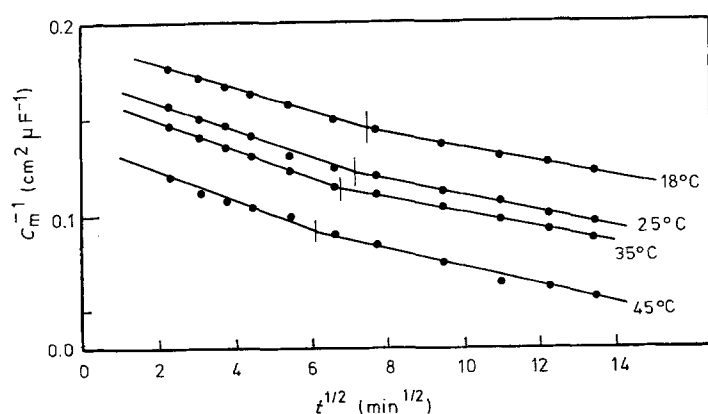

Fig. 4. Variation of the thickness of the oxide film (C_m^{-1}) with $t^{1/2}$ at different temperatures in H_2SO_4.
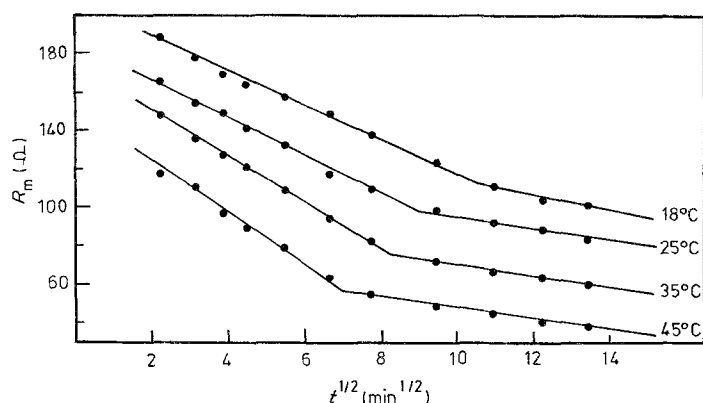
Fig. 5. Variation of the resistance of the oxide film with $t^{1/2}$ at different temperatures in H_2SO_4.

[2]. Ti exhibits three oxidation states [18]. The oxide phase close to the metal surface would seem to have an oxidation state lower than that of the outer phase. Table 1 lists values of α, α', β, β' and the ratio β/β' (α' and β' are the constants related to the dissolution of the inner layer of the oxide, that is, after the inflection point). The rate coefficient for the dissolution of the outer layer is 1.55 to 1.89 times that of the inner one. This confirms that the anodic oxide film is composed of two layers, the outer layer dissolving more readily. The outer layer, having a higher oxidation state is probably more acidic than the inner one, in addition to possessing a more defective structure which makes it more liable to dissolution. The rate determining step in the dissolution process lies within the oxide itself and may simply be the hydration of the oxide as follows

$$TiO_{2-x(s)} + H_2O_{(l)} = TiO_{2-x} \cdot H_2O_{(s)}. \qquad (2)$$
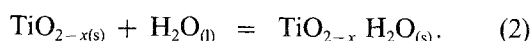
The resultant hydrated oxide is known to be slightly soluble in acid solutions, whereas the anhydrous oxide is insoluble [19].

The increase in β and β' with temperatures indicates increasing rates of dissolution of both layers with increasing temperature. This is probably due to an increase in the rate of the hydration step represented by Equation 2. Further, it is clear that β is affected by temperature more than β', and hence the increase in the ratio β/β', which is probably due to the porous nature of the outer layer, as compared to the compact structure of the inner layer.

Values of α (Table 1) depend on temperature. The initial film is similar since it has been prepared under the same experimental conditions. The differences are mainly due to the relative conductivity of the test solutions at various temperatures. The difference $\alpha-\alpha'$ (Table 1) is nearly constant, which is reasonable as the thickness of the outer layer is the same.

The inverse relation between R_m and C_m has been considered previously [20] and attributed to the properties of the electrical analogue of the series equivalent circuit. This relation is obvious when comparing Figs 4 and 5. R_m decreases linearly with $t^{1/2}$ and temperature. The inflections appear at time intervals following the same sequence as in Fig. 4, for although R_m is a direct function of the oxide thickness [21–23], it is less sensitive index than capacitance. The variation of R_m with $t^{1/2}$ can be represented by a relation similar to Equation 1. The difference in the values of R_m at zero time is clearly due to the conductance of the solutions which increase with temperature.

The results in Figs 4 and 5 indicate that the dissolution of Ti is influenced by temperature in acid medium; similar observations were reported for Zr [12] and W [24]. Arrhenius plots for the rate of dissolution were obtained at different C_m^{-1} values, Fig. 6. The activation energy, $-\Delta H$, estimated from these plots by using the relation [25]

$$RT[\mathrm{d} \ln (-C_m^{-1})/\mathrm{d}t]_{C_m^{-1}} = -\Delta H \qquad (3)$$

is $110.5\,kJ\,mol^{-1}$. This is comparable to $62.8\,kJ\,mol^{-1}$ reported for the dissolution of amorphous tungsten oxide in 0.05 M H_2SO_4 [26], and somewhat higher than $38.2\,kJ\,mol^{-1}$ reported for the dissolution of zirconium in 0.5 M H_2SO_4 [12]. This may explain why Zr does not equal Ti in resisting dissolution in certain solutions, although the corrosion resistance of Zr in most of the environments is higher than that of Ti [13].

The potential e_h, is also a direct function of the oxide thickness [21–23], although it is a less sensitive index than the capacitance for the detection of

Table 1. Dissolution coefficients in Equation 1 as a function of temperature

T ($^\circ C$)	α ($cm^2\,\mu F^{-1}$)	$10^3 \times \beta$ ($cm^2\,\mu F^{-1}\,m^{-1/2}$)	α' ($cm^2\,\mu F^{-1}$)	$10^3 \times \beta'$ ($cm^2\,\mu F^{-1}\,min^{-1/2}$)	β/β'
18	0.192	6.2	0.144	4.0	1.55
25	0.174	7.8	0.122	4.2	1.71
35	0.164	8.0	0.115	4.3	1.86
45	0.139	8.5	0.092	4.5	1.89

$\alpha' = C_m^{-1}$ at the inflection point (Fig. 4).
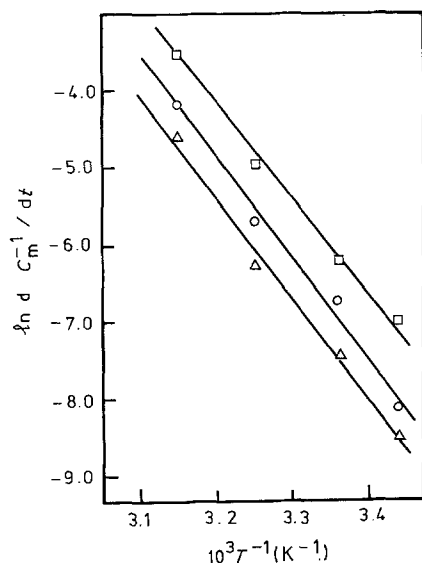
Fig. 6. Arrehenius plots at different C_m^{-1} values: △ 0.130, ○ 0.147, □ 0.170 cm² μF⁻¹.

Fig. 7. Plots of potential against the square root of time of immersion of the electrode at differrent temperatures.

variation in the electrode reaction when the electrochemical insulating properties of the film are high [23]. e_h increases with the insulating properties, that is, the thickness of the oxide film [27]. Variation of e_h with $t^{1/2}$ is shown in Fig. 7, at different temperatures. The results are in good agreement with those in Figs 4 and 5. The sequence in the time of the inflection point is the same, and an increase in the slope of both segments of the relation with increasing temperature is also observed. The slope of the first segment is higher than that of the second segment. The relation shown in Fig. 7 may be represented by

$$e_h = a - bt^{1/2} \qquad (4)$$

where a and b are constants. The minus sign indicates a decrease in e_h, that is, film thinning due to a decrease in the electrochemical insulating properties of the film [23]. The bulk properties of the oxide in H_2SO_4 undoubtedly affect the behaviour of the oxide at open circuit.

From Fig. 8, which shows the variation in both b' and β' (dissolution coefficients of the inner layer obtained from Equations 1 and 4) with temperature, it is obvious that there is some difference in the slope of the two relations. A similar observation was made for
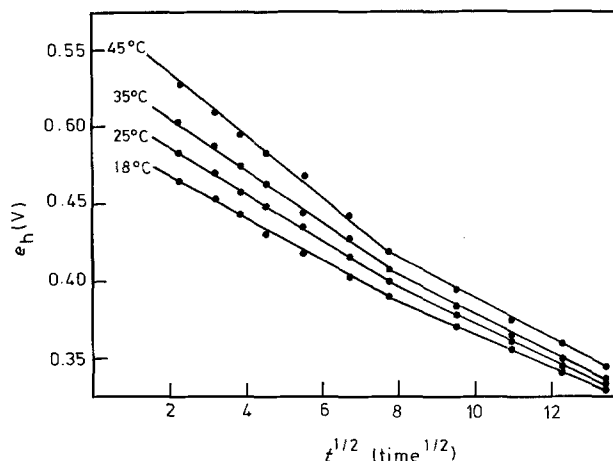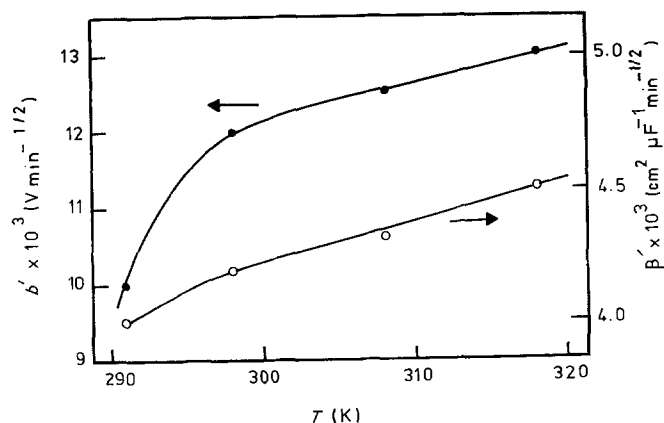
the variation of b and β with temperature. β' pertains to the rate of oxide thinning only, whereas b' may, in addition, be related to the bulk properties of the oxide. This may be through δ, the width of the energy barrier surmounted by the ion during transfer. From Fig. 8, we may infer that δ is much higher at $T = 10°$ C; with increasing temperature it decreases to a more or less constant value, so that the course of the two relations differs in the portions of the curves representing data at 18° to 25° C.

The results obtained from e_h measurements agree with those shown in Figs 4 and 5. The low coefficients of dissolution at lower temperatures are partly due to the difficulty encountered by the ion in surmounting the energy barrier during transfer, in addition to the expected decrease in the chemical dissolution with decrease in temperature.

References

[1]   M. W. Latimer, 'The Oxidation States of the Elements and their Potentials in Aqueous Solutions', 2nd edn, Prentice Hall, Englewood Cliffs, N.J. (1953) p. 266.

[2]   H. C. Gatos (Ed.), 'The Surface Chemistry of Metals and Semiconductors', Wiley, New York (1965) pp. 382 and 460.

[3]   M. E. Sibert, J. Electrochem. Soc. 110 (1963) 65.

[4]   M. S. El-Basiouny and A. A. Mazhar, Corrosion 38 (1982) 237.

[5]   M. M. Hefny, A. A. Mazhar and M. S. El-Basiouny, Br. Corros. J. 17 (1982) 38.

Fig. 8. Variation of the constants b' and β' with temperature.

[6] A. A. Mazhar, M. M. Hefny, F. El-Taib Heakal and M. S. El-Basiouny, *ibid.* **18** (1983) 156.
[7] V. V. Andreeva, *Corrosion* **20** (1964) 35t.
[8] E. Ence and J. Margolin, *J. Metals* **6** (1954) 346.
[9] J. S. Llewelyn Leach and B. R. Pearson, *Electrochim. Acta* **29** (1984) 1263.
[10] M. W. Breiter, *Electrochim. Acta* **15** (1970) 1195.
[11] K. S. Yun, S. M. Wilhelm, S. Kapusto and N. Hackerman, *J. Electrochem. Soc.* **127** (1980) 85.
[12] M. S. El-Basiouny, A. A. Mazhar, F. El-Taib Heakal and M. A. Ameer, *J. Electroanal. Chem.* **147** (1983) 181.
[13] J. A. Petit, G. Chatainier and F. Dabosi, *Corros. Sci.* **21** (1981) 279.
[14] L. C. Archibald and J. S. L. Leach, *Electrochim. Acta* **22** (1977) 21.
[15] T. Ohtsuka, M. Masuda and N. Sato, *J. Electrochem. Soc.* **132** (1985) 787.
[16] B. Maurel, D. Diemegard and G. Amsel, *J. Electrochem. Soc.* **119** (1972) 1715.
[17] A. A. Mazhar, F. El-Taib Heakal and A. S. Mogoda, *Corrosion* **44** (1988) 322.

[18] R. I. H. Clark, 'Comprehensive Inorganic Chemistry', Vol. 3, Pergamon Press, Oxford (1973) Chap. 32.
[19] M. Pourbaix, 'Atlas of Electrochemical Equilibria in Aqueous Solutions', Pergamon Press, Oxford (1966) p. 213.
[20] M. S. El-Basiouny, A. M. El-Kot and M. M. Hefny, *Br. Corros. J.* **14** (1979) 51.
[21] J. M. Abd El-Kader, F. M. Abd El-Wahab, H. A. El-Shayeb and M. G. A. Khedr, *ibid.* **16** (1981) 111.
[22] J. M. Abd El-Kader and A. M. Shams El-Din, *ibid.* **14** (1979) 40.
[23] A. M. Bekheet, M. M. Hefny, A. A. Mazhar and M. S. El-Basiouny, *Annls. Chim. (Rome)* **73** (1983) 63.
[24] A. Dipoala, F. D. Quarto and C. Sunseri, *J. Electrochem. Soc.* **125** (1978) 1344.
[25] J. O'M. Bockris and E. C. Potter, *J. Chem. Phys.* **20** (1952) 614.
[26] A. T. Vas'ko and V. V. Tobolich, *Dopov. Adad. Nauk. Ukr. R.S.R. Ser. B.* **33** (1971) 706.
[27] A. K. Vijh, *Corros. Sci.* **12** (1972) 105.